Proceedings of the XVII ECSMGE-2019
Geotechnical Engineering foundation of the future
ISBN 978-9935-9436-1-3

doi: 10.32075/17ECSMGE-2019-1005

XVII European Conference
ECSMGE 2019
Reykjavik
on Soil Mechanics
and Geotechnical Engineering

Effects of a multi-directional loading sequence on offshore wind turbine natural frequencies

Effet d'un chargement multi-directionnel sur le calcul de fréquence propre d'une éolienne en mer

A. Lovera
EDF R&D, Saclay, France
Laboratoire Navier, Ecole des Ponts ParisTech, IFSTTAR, CNRS, Champs-sur-Marne, France

S. Ghabezloo, J. Sulem
Laboratoire Navier, Ecole des Ponts ParisTech, IFSTTAR, CNRS, Champs-sur-Marne, France

M. F. Randolph
Centre for Offshore Foundation Systems, Perth, Australia

M. Kham
EDF R&D, Saclay, France

E. Palix
EDF Renouvelables, La Defense, France

ABSTRACT: The evaluation of the natural frequencies of offshore wind turbines is a key design criterion. It is commonly based on the definition of a macro-element representing the response of the foundation which is assessed on the basis of the *P-y* curves approach for laterally loaded pile. The existing framework of *P-y* curve formulation is limited to a single direction of loading. However, for offshore wind turbines the directions of the lateral loads may vary due to the effects of wind and waves. Based on a recent extension of the *P-y* curves framework proposed by the authors, the impact of multi-directional loading on natural frequency analysis of an offshore wind turbine with a monopile as foundation is studied. It is shown that a loading-sequence with multi-directional loading may lead to a decrease of natural frequencies of around 3-5 % depending on the orientation of successive loadings.

RÉSUMÉ: La détermination des fréquences propres des éoliennes en mer est un critère important lors du dimensionnement. Elle est généralement basée sur la définition d'un macro-élément représentant la réponse de la fondation au niveau de la surface du sol. Ce macro-élément est évalué en utilisant l'approche des courbes *P-y*. La méthode existante des courbes *P-y* suppose que la charge est toujours appliquée dans une unique direction. Cependant, pour les éoliennes en mer, les charges latérales qui s'appliquent peuvent changer de directions en raison des effets du vent et des vagues. Basé sur un cadre généralisé proposé par les auteurs, l'étude de l'effet d'un chargement multi-directionnel sur l'analyse fréquentielle d'une éolienne en mer fondée avec un monopieu est réalisée. Une séquence de chargement avec un changement de direction entre deux chargements peut conduire à une diminution de l'ordre de 3-5 % des fréquences propres de l'éolienne.

Keywords: Laterally loaded pile, Multi-directional loading, *P-y* curves, Windmills

1 INTRODUCTION

There are several examples of civil engineering structures with pile foundations subjected to loads with varying directions (offshore and onshore wind turbines …). The design of pile foundations for these kinds of structure is generally carried out assuming that the load is acting in only one direction (DNV, 2014). Figure 1 shows that the loading from wind and waves at Hornsea wind farm in the North Sea is far from being uni-directional and indicates the order of magnitude of the range of possible misalignments between two loadings. These data are of course site dependent.

There have been several experimental studies that explored the effects of multi-directional loading on piles. In the context of large-diameter piles for offshore wind turbines (OWT), these include test results presented in Peralta (2010) and in Rudolph et al. (2014). Both studies were based on piles at reduced scale, focusing on cyclic response and the impact of multi-directional loading on accumulation of displacements. The conclusions from the studies were rather different perhaps due to the fact that the loading regimes considered were quite different. Rudolph et al. (2014) found that changes in loading direction gave significantly increased accumulation of displacements compared to uni-directional loading; by contrast Peralta (2010) showed that it was conservative in terms of accumulation of displacements to consider uni-directional loading.

Accumulation of displacements, and especially rotation, is a critical design criterion to check during design of OWTs (DNV, 2014), but an other important design criterion consists of the natural frequency range of the monopile and turbine system. The response of the structure depends closely on the first natural frequency (Kallehave et al., 2015). OWTs are dynamically loaded structures subjected to operational and environmental loads. They are commonly designed so that they do not enter in resonance, avoiding rotor and blade frequencies and those of

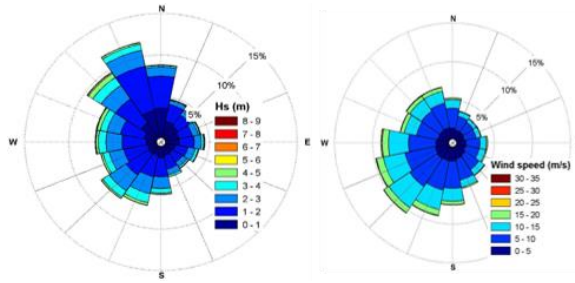

Figure 1. Wind rose (left) and wave rose (right) at Hornsea wind farm, from National Infrastructure Planning (https://infrastructure.planninginspectorate.gov.uk/)

wave and wind loading. This can be very challenging as the allowed frequency window can be very narrow. Differences between the designed natural frequency and that measured have been reported in the literature (Arany et al., 2015 and Kallehave et al., 2015). A decrease of the natural frequency after a few months has also been reported in Arany et al. (2015).

There are various methods available to calculate the behaviour of a laterally loaded pile but little attention has been paid to multi-directional loading effects. An energy-based variational approach was presented in Levy et al. (2007). Recently, Lovera et al. (2018) proposed an extension of the *P-y* curve approach permitting consideration of multi-directional effects. This model is used here for the application case.

The outline of the paper is as follows. First, the multi-directional model is described briefly. In section 3, an application case is presented on the effect on multi-directional loading on the macro-element used to model the whole foundation of an OWT in natural frequency analysis. The results of a sensitivity study are discussed.

2 MODEL DEFINITION

A brief description of the multi-directional model is given here. More details can be found in Lovera et al. (2018). In order to model multi-directional effects, several springs are considered around the perimeter of the pile instead of only one spring for the uni-directional model. Figure 2

shows a section of pile with 8 springs around its perimeter. Similarly to the uni-directional model two diametrically opposed spring cannot be activated at the same time. We assume that N springs are distributed around the pile circumference, with N a multiple of 4.

Neglecting torsion and assuming no axial friction along the pile, momentum balance of an infinitesimal pile element of length dz leads to the following differential system:

$$\begin{cases} \frac{\mathrm{d}^2}{\mathrm{d}z^2}\left(\left(E_p I_p\right)_x \frac{d^2x}{\mathrm{d}z^2}\right) + V\frac{\mathrm{d}^2x}{\mathrm{d}z^2} + P_x(x,y) = 0 \\ \frac{\mathrm{d}^2}{\mathrm{d}z^2}\left(\left(E_p I_p\right)_y \frac{d^2y}{\mathrm{d}z^2}\right) + V\frac{\mathrm{d}^2y}{\mathrm{d}z^2} + P_y(x,y) = 0 \end{cases} \quad (1)$$

In the above equations, x and y are the displacements in two perpendicular directions of the pile, $\left(E_p I_p\right)_x$ and $\left(E_p I_p\right)_y$ are the flexural rigidities in the two directions, z is the vertical coordinate along the pile, V is the vertical force applied on top of the pile and P_x and P_y are the soil reactions mobilized in the two perpendicular directions.

2.1 Hyperbolic tangent P-y curve

In the uni-directional *P-y* curve method, a series of springs are placed along the depth of the pile. Each spring represents a (non-linear) *P-y* response. Various *P-y* curves can be found in the literature for various type of soil. In the multi-directional model, a given loading activates several springs around the pile diameter. This section summarises the equations developed in Lovera et al. (2018) to establish new expressions for *P-y* curves in the multi-directional model in the case of hyperbolic function *P-y* curves.

Assuming a tangent hyperbolic function for the *P-y* curve, such as recommended for sandy soils in API (2000) for example, the following notations and expressions are used:

$$P(y) = P_u \tanh\frac{ky}{P_u} \quad (2a)$$

$$\tilde{P}(y) = \widetilde{P_u} \tanh\frac{\tilde{k}y}{\widetilde{P_u}} \quad (2b)$$

where the tilde symbol is used for each corresponding value in the multi-directional model. This kind of *P-y* curve has two parameters: the initial stiffness k and the ultimate reaction P_u. In order to have the same global response as the uni-directional model considering a single loading, these parameters should satisfy the following equations (Lovera et al., 2018):

$$\tilde{k} = \frac{4k}{N} \quad (3)$$

$$\widetilde{P_u} = P_u \tan\frac{\pi}{N} \quad (4)$$

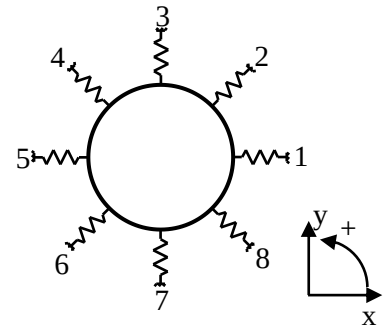

Figure 2. Example of a pile section in a multi-directional model with N equal to 8.

2.2 Irreversible response

The *P-y* curves are usually assumed to be reversible (e.g DNV, 2014). This simplified assumption might not be relevant for real situations. In order to take into-account the irreversible behaviour of the soil an unloading path is defined for each spring. It is assumed that the slope of the unloading path is given by the initial stiffness of the corresponding (*P-y*) curve. In the case of gapping between the pile and the ground, the pile moves freely towards its initial position (zero displacement) without mobilizing the soil reaction, before starting to mobilize the diametrically opposite spring.

3 APPLICATION FOR OWT NATURAL FREQUENCY ANALYSIS

The presented application case focuses on the impact of multi-directional loading on natural frequency analysis. The publicly available characteristics of the 5 MW wind turbine developed by National Renewable Energy

Laboratory (NREL) are used in this application case. The monopile configuration is considered. The methodology consists in first defining a macro-element representing the foundation which was subjected to a multi-directional loading sequence. In a second step, this macro-element is used as an input parameter for the natural frequency analysis.

The problem is first described in terms of geometry and soil conditions. The soil conditions are used to derive the macro-element whereas the tower geometry and turbine characteristics are used for the natural frequency analysis. Then, the loading path used to derive the macro-element is presented, taking account of the impact of multi-directional loading. The assumptions for the macro-element are discussed and finally, the results of a sensitivity study are presented.

3.1 Studied problem

3.1.1 Geometry and soil conditions

The NREL 5-MW turbine is considered. The properties needed for the analysis can be found in Jonkman et al. (2009). The mass of the rotor-nacelle assembly (RNA) is taken to be 350 000 kg. The RNA inertias are assumed equal to $2.35\times10^7\,\mathrm{m}^4$ in the fore-aft plane and $4.35\times10^7\,\mathrm{m}^4$ for side-side motion (cf. Figure 3).

The structure is modelled using Euler beam elements with characteristics of the tower given in Jonkman and Musial (2010). The diameter and the thickness of the tower are assumed to be linearly tapered from base to top.

The configuration with monopile in a sandy ground is considered here with the soil-pile-interaction model as described in Passon (2006). The layered soil conditions considered are described in Table 1 assuming the hyperbolic tangent formulation of the API-sand model (API, 2000). The initial stiffness and ultimate reaction vary with depth and are expressed as (API, 2000):

$$k = k_y z \tag{5}$$

$$P_u = 0.9\,\min[(C_1 z + C_2 D)\gamma' z; C_3 D\gamma' z] \tag{6}$$

where k_y is the rate of increase of the subgrade reaction modulus, z the considered depth below ground level, C_1, C_2 and C_3 dimensionless constants depending on friction angle φ, D the pile diameter and γ' the soil effective weight. These parameters are deduced for the multi-directional loading using Equations 3 and 4 and considering 36 springs around the pile periphery (one spring every 10°).

Table 1. Properties of the soil layered considered (after Passon, 2006)

	Layer 1	Layer 2	Layer 3
Layer top	0 m	5 m	14 m
Layer bottom	5 m	14 m	∞
Effective limit weight γ’	10 kN/m^3		
Friction angle φ	33°	35°	38.5°
P-y modulus k_y [kN/m^3]	16287	24430	35288

For the frequency analysis, we model the macro-element considering the same loading conditions as in Passon (2006). These consist of a lateral load of 3910 kN and a bending moment of 124385 kN.m, and thus a lever arm of 32 m. Considering a lever arm of 32 m and the given *P-y* curves (Equation 2a) an ultimate lateral load of around 50 MN may be deduced with a corresponding bending moment of 1600 MN.m. In the following the loading is expressed as a ratio of the ultimate lateral load.

3.1.2 Loading path

The following loading sequence is considered for the macro-element calculation:

- *stage I*: loading in the *x*-direction with a combined force and moment;
- *stage II*: unloading in the *x*-direction to zero load and zero moment;

- *stage III*: loading with a combined force and moment defined as representative loading in Passon (2006) at an angle ψ to the *x*-direction.

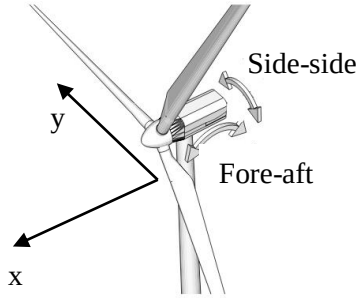

Figure 3. Sketch showing directions of fore-aft and side-side modes on a wind turbine (after Knudsen et al. 2012)

3.1.3 Macro-element assumptions

The macro-element modelling consists in representing the whole foundation response below ground level with one stiffness matrix. In natural frequency analysis, we are only interested in small displacements and rotations (Bhattacharya and Adhikari, 2011) so that a linearisation of the response of the foundation is performed for the assumed pre-loaded conditions.

In the case of monopiles for offshore wind turbines subjected mainly to lateral loading, the stiffness terms related to the degrees of freedom of vertical displacement and torsion are usually not considered. For a uni-directional loading the stiffness matrix of the macro-element (Equation 7) is symmetric and includes coupling terms between displacement in a given direction and the corresponding rotation. These coupling terms *have a non-negligible effect on the natural* frequency analysis (Arany et al., 2015).

$$\begin{bmatrix} F_x \\ F_y \\ M_x \\ M_y \end{bmatrix} = \begin{bmatrix} K_{LL} & 0 & 0 & -K_{LR} \\ 0 & K_{LL} & -K_{LR} & 0 \\ 0 & -K_{LR} & K_{RR} & 0 \\ -K_{LR} & 0 & 0 & K_{RR} \end{bmatrix} \begin{bmatrix} x \\ y \\ \theta_x \\ \theta_y \end{bmatrix} \quad (7)$$

where K_{LL}, K_{RR} and K_{LR} are the lateral, rotational and cross-stiffness terms for the uni-directional model respectively. Note that for symmetry reasons the lateral stiffnesses in *x* and *y*-directions are equal as well as the rotational ones. Using the uni-directional model, the representative loads defined in Passon (2006) and the soil properties given in Table 1, we find $K_{LL} = 1.87 \times 10^9$ N/m, $K_{RR} = 1.95 \times 10^{11}$ N.m and $K_{LR} = 1.54 \times 10^{10}$ N.

When multi-directional effects are considered., the stiffness matrix is no longer symmetric since the soil stiffness in the direction of a previous loading is altered. The general form of the stiffness matrix of the macro-element is:

$$\begin{bmatrix} F_x \\ F_y \\ M_x \\ M_y \end{bmatrix} = \begin{bmatrix} K_{xx} & K_{xy} & K_{x\theta_x} & K_{x\theta_y} \\ K_{yx} & K_{yy} & K_{y\theta_x} & K_{y\theta_y} \\ K_{\theta_x x} & K_{\theta_x y} & K_{\theta_y\theta_y} & K_{\theta_x\theta_y} \\ K_{\theta_y x} & K_{\theta_y x} & K_{\theta_y\theta_x} & K_{\theta_y\theta_y} \end{bmatrix} \begin{bmatrix} x \\ y \\ \theta_x \\ \theta_y \end{bmatrix} \quad (8)$$

where K_{XY} in the above matrix is equivalent to the force or moment X to apply corresponding to a displacement of 1 m or a rotation of 1 rad of the degree of freedom Y while the other degrees of freedom are equal to zero. Additional extra-diagonal terms appear when considering multi-directional loading. For example, an applied force in the *x*-direction, leads not only to a displacement along the *x*-axis and a rotation around the *y*-axis, but also to a displacement along the *y*-axis and a rotation around the *x*-axis.

3.2 Results and sensitivity study

The methodology presented in the previous section is implemented and a sensitivity study is performed. The parameters that are considered to vary are: the level of loading applied during stage I, and the angle ψ of the direction of loading (counter clockwise from the *x*-axis).

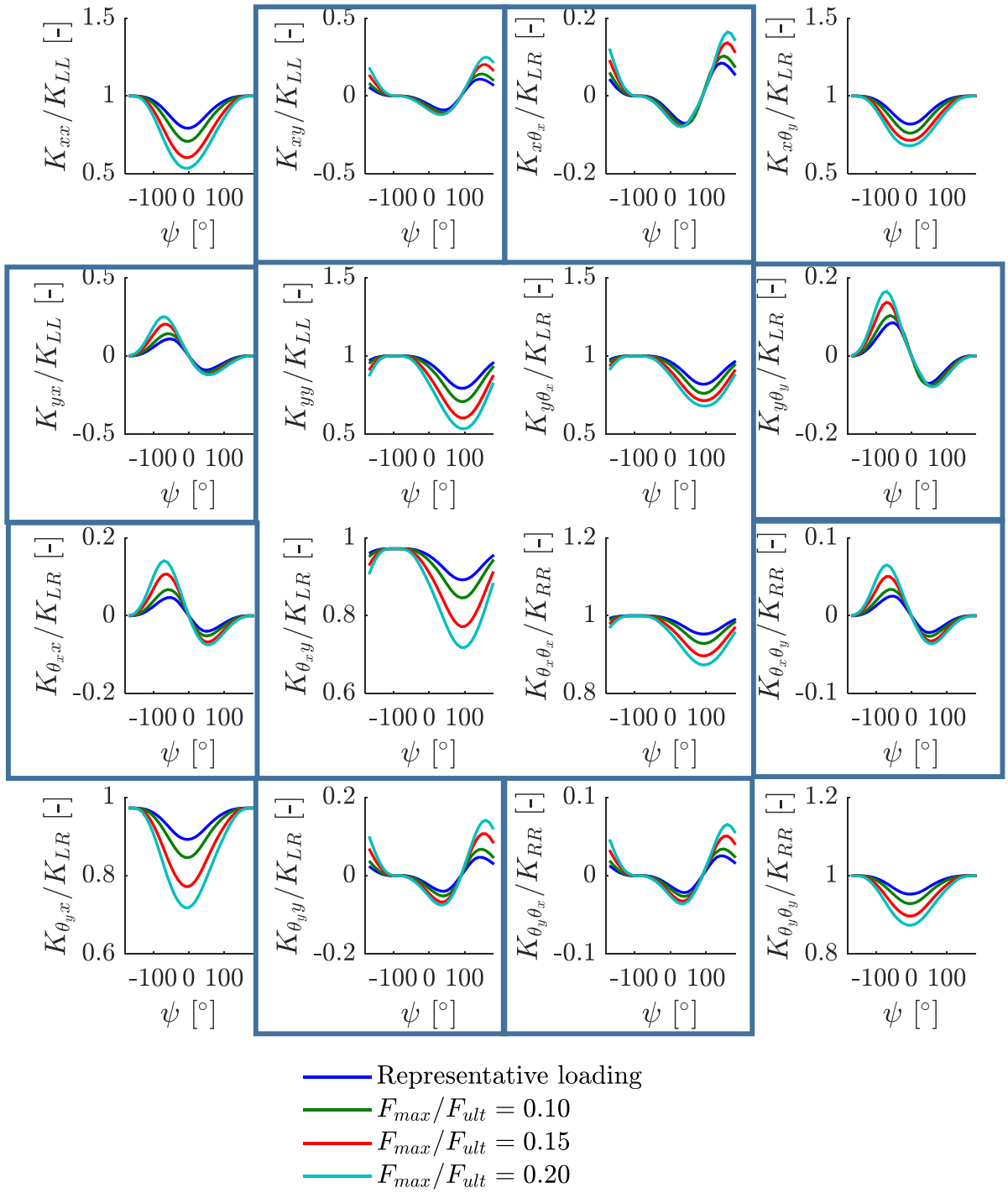

Figure 4. Stiffness matrix of the macro-element: Effect of the angle of loading in stage III on the stiffness matrix terms of the macro-element for various maximum loads previously experienced in stage I. Solid frames correspond to the additional coupling terms due to multi-directional effects.

Figure 4 shows the dependency of the stiffness matrix of the macro-element with the angle of loading during stage III for different ratios of ultimate load experienced during stage I. For a clearer demonstration of the effects of multi-directional, each term of the stiffness matrix is normalized with respect to either K_{LL}, K_{RR} or K_{LR}, depending on the unity of the considered term. It can be seen that the evolution of the lateral stiffness K_{xx} and K_{yy} with the loading direction are identical and just shifted by 90°. The same observation holds for the evolution of $K_{\theta_x\theta_x}$and $K_{\theta_y\theta_y}$, and for the evolution of $K_{x\theta_y}$ and $K_{y\theta_x}$. Note that the terms corresponding to x and y directions are different as opposed to the uni-directional case. Consequently, the fore-aft and the side-side natural frequency evolve differently.

The effect of the multi-directional loading experienced during the loading sequence is a decrease of all the terms of the stiffness matrix as compared to the uni-directional model. For example, considering an initial loading during stage I of 20% of the ultimate load, and depending on the loading direction in stage III, the lateral stiffness can be reduced up to 50%, the cross-coupling terms up to 70% and the rotational stiffness up to 88%.

The frequency analysis is performed on the macro-element obtained for given loading conditions as described above. As an example, we consider an applied loading in phase I that corresponds to either the representative loads or to 10, 15 and 20% of the ultimate loading applied in x-direction and evaluate the natural frequencies of the OWT for an arbitrary loading direction ψ in phase III. Figure 5 shows the dependence of 1st and 2nd mode natural frequencies (for-aft and side-ide) with the loading direction. We observe that the minimum side-side frequencies are shifted of 90° as compared for the fore-aft frequencies. Therefore, for a given loading direction ψ, one frequency is more altered than the other. For example, a previous applied loading of 20% of ultimate can lead to a decrease of fore-aft (respectively side-side) frequency of around 3.5% (resp. 2%) for the first mode and around 4.5% (resp. 1%) for the second one. The figure also shows that the fore-aft natural frequency is more impacted than the side-side frequency, which is due to the fact that the loading in stage I was parallel to the x-axis (fore-aft direction).

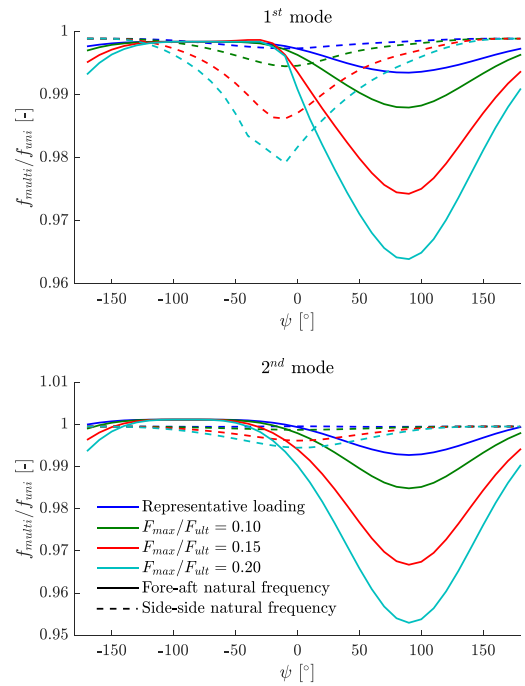

Figure 5. Evolution of first (top) and second (bottom) mode for fore-aft (solid lines) and side-side (dashed lines) natural frequencies with angle of multi-directional loading for various maximum load levels experienced

4 CONCLUSIONS

In this paper, we explore the effects of multi-directional loading on the natural frequencies of OWTs using an extension of the load transfer (*P-y* curve) approach to include the effects of multi-directional loading. The frequency analysis is based on the definition of a macro-element which accounts for pre-loaded conditions. The effects of the multi-directional loading have been

illustrated through the loss of symmetry and a reduction of all the terms in the stiffness matrix of the macro-element. Moreover, this loss of symmetry results in additional coupling effects between the direction of loading and lateral and rotational stiffness in other directions. An application to the evaluation of the natural frequencies of an OWT demonstrates that multi-directional loading leads to a reduction of a few percent of the 1st and 2nd modes frequencies. This could be (at least to some extent) a possible explanation of the shifting of the natural frequency as mentioned by Arany et al. (2015) during the first few months after installation, in addition to softening effects of the surrounding soil.

5 ACKNOWLEDGEMENTS

The author would like to thank Parc du Banc de Guérande and Eoliennes en Mer du Calvados projects for the authorization to publish this article. The fourth author is grateful for support through the Centre for Offshore Foundation Systems, until recently a node of the Australian Researh Council Centre of Excellence in Geotechnical Science and Engineering (CE110001009).

6 REFERENCES

API. 2000. *Recommended practice for planning, designing and constructing fixed offshore platforms – Working stress design*, 21st edition, API-RP-2A-WSD.

Arany, L., Bhattacharya, S., Adhikari, S., Hogan, S.J., Macdonald, J.H.G. 2015. An analytical model to predict the natural frequency of offshore wind turbines on three-spring flexible foundations using two different beam models. *Soil Dynamics and Earthquake Engineering* **74**, 40-45

Bhattacharya, S., Adhikari, S. 2011. Experimental validation of soil-structure interaction of offshore wind turbine, *Soil Dynamics and Earthquake Engineering* **31**, 805-816

DNV. 2014. Offshore standard DNV-OS-J101, Design of offshore wind turbine structures (last edition).

Jonkman, J., Butterfiel, S., Musial, W., Scott, G. 2009. *Definition of a 5-MW reference wind turbine for offshore system development.* NREL/TP-500-38060, Golden, CO: National Renewable Energy Laboratory.

Jonkman, J., Musial, W. 2010. *Offshore code comparison collaboration (OC3) for IEA task 23 offhsore wind technology and deployment* NREL/TP-500-48191, Golden, CO: National Renewable Energy Laboratory.

Knudsen, T., Bak, T., Tabatabaeipour, S.M. 2012. Detection of excessive wind turbine tower oscillations fore-aft and sideways, *American Control Conference*, 5795-5800.

Levy, N.H., Einav, I., Randolph, M.F. 2007. Effect of recent load history on laterally loaded piles in normally consolidated clay, *International Journal of Geomechanics* **7**, 277-286

Lovera, A., Ghabezloo, S., Sulem, J., Randolph, M., Kham, M., Palix, E. 2018. Pile response to multi-directional lateral loading using p-y curves approach, *Géotechnique*, Submitted.

Passon, P. 2006. *Memorandum derivation and description of the soil-pile-interaction models.* IEA-Annex XXIII Subtask 2, Stuttgart, Germany: Endowed Chair of Energy.

Rudolph, C., Bienen, B., Grabe, J. 2014. Effect of variation of the loading direction on the displacement accumulation of large-diameter piles under cyclic lateral loading in sand, *Canadian Geotechnical Journal* **51**, 1196-1206.